Check for updates

Human Gait Anomaly Detection Using LiDAR for Healthcare Monitoring

*Anuroop Gaddam, Muhammad Zeeshan Khan, and Dhananjay Thiruvady

School of Information Technology, Deakin University, Geelong, VIC 3216, Australia
{anuroop.gaddam, muhammad.zeeshankhan, dhananjay.thiruvady}@deakin.edu.au

Abstract. This chapter presents the AI-Driven Real-Time detection of Gait anomalies utilizing LiDAR Technology for Advanced Healthcare Monitoring. This innovative approach leverages cutting-edge artificial intelligence and sophisticated Light Detection and Ranging technology to track and analyze individuals' gait patterns in real time. By monitoring the walking patterns of movement, this system aims to identify and detect any anomalies that may indicate underlying health issues. The implementation of such a system in healthcare settings offers a novel method for continuous monitoring, contributing to early diagnosis, improved patient outcomes, and a deeper understanding of mobility-related conditions.

Keywords: LiDAR, Internet of Things (IoT), Real-Time Healthcare Monitoring, Gait Anomaly Detection, Elderly Fall Risk, Smart Health Systems

1 Data Acquisition, Processing, and Visualisation

The effective implementation of LiDAR-based healthcare monitoring systems hinges on robust data acquisition protocols, accurate calibration, and efficient processing and visualisation pipelines. These elements ensure the quality and reliability of the data used for subsequent analysis, such as activity recognition or gait assessment.

LiDAR Data Acquisition Techniques and Protocols The acquisition of high-quality LiDAR data in healthcare settings begins with careful planning and adherence to specific protocols. Sensor selection is paramount, considering factors like the required field of view, range, resolution, and eye safety (Class 1 for patient environments). The placement of LiDAR sensors is also critical: for gait analysis, sensors might be positioned at shin height to accurately capture leg movements , while for general room monitoring or fall detection, ceiling-mounted or wall-mounted positions might be preferred to provide a comprehensive view. The defined region of interest (ROI) must encompass the areas where patient activity is expected, and the sensor's effective sensing range limitations must be considered, as accuracy can degrade at the extents of its range.

N. K. Suryadevara (ed.), *Proceedings of the IoT AND LiDAR Technologies in Healthcare Workshop (ILTH 2024)*, Atlantis Highlights in Intelligent Systems 14,
https://doi.org/10.2991/978-94-6463-784-7_10

Data logging systems must be capable of reliable, high-capacity, real-time recording of the point cloud data, along with precise timestamps and any associated sensor metadata (e.g., IMU readings). For clinical studies or validation purposes, data acquisition protocols often involve standardised tasks performed by participants (e.g., specific walking patterns, simulated falls) under controlled conditions. Crucially, these protocols must include procedures for obtaining informed consent from participants and ensuring synchronisation if multiple sensors or reference systems (like motion capture or IMUs) are used for comparison. Standardisation of these acquisition protocols is vital for ensuring the comparability and reproducibility of research findings across different studies and for facilitating the development of generalisable models. Variations in sensor setup or experimental procedures can significantly impact data characteristics and algorithmic performance.

Calibration Methods for Indoor Monitoring Accurate calibration is the bedrock of any reliable multi-sensor system and is essential for precise 3D environmental mapping and patient tracking using LiDAR. Even minor calibration errors can propagate, leading to significant inaccuracies in the final analysis.

- **Multi-Sensor (LiDAR-to-LiDAR) Calibration:** When multiple LiDAR sensors are used to extend coverage or provide different perspectives, their relative positions and orientations (extrinsic parameters) must be precisely determined. This ensures that individual point clouds can be accurately merged into a common coordinate system. Calibration methods can be:
  - *Target-based:* Using objects of known geometry (e.g., checkerboards, spheres) visible to multiple sensors.
  - *Targetless:* Based on overlapping features or motion-based techniques that deduce relative alignment through sensor movement.

  Recent research explores automatic, motion- and targetless frameworks that support varied sensor alignments, provided their fields of view overlap.
- **LiDAR-Camera Calibration:** Required when fusing LiDAR data with camera information (e.g., for texture mapping or visual question answering). This involves computing the extrinsic transformation between the two sensor coordinate systems, typically after intrinsic camera calibration (e.g., estimating focal length and distortion).
- **Best Practices for Indoor Calibration and Mapping:**
  - Move slowly and steadily during mobile scans to avoid errors in SLAM algorithms.
  - Ensure consistent lighting for camera-based systems.
  - Avoid or cover highly reflective surfaces like mirrors or metal to prevent false LiDAR reflections.
  - Minimise SLAM drift by scanning in smaller overlapping sections or forming loops to allow correction.
  - Ensure temporal synchronisation across all sensors to align data to the same time frame.
  - Correct extrinsic errors to prevent point cloud misalignment, ghosting, and inaccurate spatial measurements.

Role of ROS, Open3D, and RViz in Data Handling The development and implementation of LiDAR-based healthcare applications are significantly accelerated by powerful open-source tools for data handling, processing, and visualisation:

- **Robot Operating System (ROS):** A flexible, modular framework used well beyond robotics. ROS offers:
  - **Sensor Integration:** ROS provides drivers for a wide range of LiDAR sensors, publishing standardised message types such as `sensor msgs/_LaserScan` (2D) and `sensor_msgs/PointCloud2` (3D).
  - **Data Communication:** ROS uses a publish-subscribe model for inter-node communication and services for synchronous requests.
  - **Real-Time Processing:** ROS enables real-time data processing pipelines for sensor data.
  - **SLAM and Navigation:** ROS includes packages such as GMapping and Cartographer for Simultaneous Localisation and Mapping (SLAM) and autonomous navigation.
  - **Data Logging and Playback:** The `rosbag` utility records and replays all ROS topic data (e.g., LiDAR, IMU, outputs), facilitating debugging and reproducibility.
- **Open3D:** An open-source C++/Python library tailored for 3D data. It supports:
  - **Point Cloud Manipulation:** Operations such as downsampling (e.g., voxel grid), denoising, normal estimation, and computing geometric descriptors like FPFH.
  - **Registration:** Implements algorithms like Iterative Closest Point (ICP) and RANSAC-based methods for scan alignment.
  - **Segmentation:** Rule-based and learning-based segmentation of point clouds.
  - **Visualisation:** Interactive 3D viewer for inspecting LiDAR scenes. Often integrated with ROS pipelines for on-the-fly analysis.
- **RViz:** The native 3D visualisation tool in ROS, used to display:
  - Raw 2D LiDAR scans and 3D point clouds.
  - Robot URDF models and associated coordinate frames (TFs).
  - Maps generated from SLAM modules.
  - Outputs from perception algorithms such as tracked people or obstacle detections.

  RViz provides real-time updates, colour customisation, and overlays for debugging and demo purposes. Alternatives like Foxglove offer similar capabilities with enhanced interfaces and web-based compatibility.

These open-source platforms significantly lower the barrier to entry for research and development in LiDAR-based healthcare. They provide robust, prebuilt functionalities for many common tasks, allowing researchers to focus on the novel aspects of their healthcare applications rather than developing foundational infrastructure from scratch.

The following table (Table 1.1) provides a comparative overview of different LiDAR technologies relevant to healthcare applications.

Table 1: Comparison of LiDAR Technologies for Healthcare Applications

Feature	**2D LiDAR**	**3D LiDAR**	**Discrete Return LiDAR**	**Full Waveform LiDAR**
Dimensionality	Scans a single plane (horizontal/vertical)	Scans in three dimensions	Records distinct reflection points	Records entire reflected energy waveform
Data Output	2D point cloud / line scan	3D point cloud	Set of (X, Y, Z) points per pulse	Continuous waveform data per pulse
Complexity (Data)	Lower	Higher	Moderate	High
Complexity (Processing)	Lower	Higher	Moderate	High
Cost	Generally lower	Generally higher	Varies	Varies, often higher due to data volume
Typical Healthcare Use Cases	Basic gait analysis (ankle tracking), simple obstacle detection, robot navigation	Comprehensive activity recognition, fall detection in complex scenes, detailed environmental mapping, advanced gait analysis	Surface detection, object boundary identification	Detailed structural analysis, potential for analysing occluded parts or material properties

2 LiDAR for Gait Anomaly Detection

Gait, the manner or style of walking, is a complex biomechanical process that serves as a critical indicator of an individual's overall health and functional status. Deviations from normal gait patterns, known as gait anomalies, can be early signs of various underlying medical conditions, particularly neurological disorders, musculoskeletal issues, or an increased risk of falls. LiDAR technology is emerging as a powerful tool for the objective, quantitative, and non-intrusive assessment of gait, offering the potential to detect subtle anomalies that might be missed by subjective observation or less frequent clinical assessments. This section will explore the fundamentals of human gait, the clinical relevance of gait parameters, the design of LiDAR-based gait analysis systems, the application of deep learning techniques for anomaly detection, and the methods for evaluating system performance.

Fundamentals of Human Gait: Biomechanics and Key Gait Cycle Phases A thorough understanding of normal human gait biomechanics is foundational for identifying and interpreting anomalies. The human gait cycle is a repetitive sequence of limb movements that begins when one foot makes initial contact with the ground and ends when the same foot contacts the ground again. It is broadly divided into two main phases: the stance phase and the swing phase.

Gait Phases and Sub-Phases The human gait cycle is typically divided into two major phases: the stance phase and the swing phase. Each phase has distinct sub-phases that are clinically and biomechanically relevant.

- **Stance Phase:** This phase constitutes approximately 60% of a single gait cycle and occurs when the foot is in contact with the ground. It is responsible for supporting body weight, absorbing shock, and providing propulsion. It is further subdivided into:
  1. **Initial Contact (Heel Strike):** The moment the heel (or another part of the foot) first touches the ground. The objective is to initiate weight acceptance and decelerate the limb.
  2. **Loading Response (Foot Flat):** From initial contact until the contralateral (opposite) foot lifts off the ground. The foot becomes flat on the ground, absorbing impact and accepting body weight.
  3. **Mid-Stance:** Begins when the contralateral foot is lifted and continues until the body weight is aligned over the forefoot of the stance limb. The body is supported by a single leg, and stability is crucial.
  4. **Terminal Stance (Heel Off):** Begins when the heel of the stance limb lifts off the ground and continues until the contralateral foot makes initial contact. This phase initiates forward propulsion.
  5. **Pre-Swing (Toe Off):** From initial contact of the contralateral limb until the toes of the stance limb lift off the ground. The limb is rapidly unloaded, and the final push-off occurs.

– **Swing Phase:** This phase constitutes approximately 40% of the gait cycle, during which the foot is not in contact with the ground and the limb advances forward. The primary objectives are limb advancement and foot clearance to avoid tripping. It is further subdivided into:
  1. **Initial Swing:** Begins when the foot lifts off the ground and continues until maximum knee flexion occurs. The swinging foot is opposite the stance foot and is lifted clear of the ground.
  2. **Mid-Swing:** From maximum knee flexion until the tibia of the swinging leg is vertical or perpendicular to the ground. The limb continues to advance.
  3. **Terminal Swing (Deceleration):** Begins when the tibia is vertical and ends when the foot makes initial contact with the ground. The limb decelerates in preparation for heel strike.

During the gait cycle, there are also periods of double support, where both feet are simultaneously in contact with the ground (occurring during the loading response of one limb and the pre-swing of the other). The duration of these phases and the kinematics (joint angles, velocities, accelerations) of the ankle, knee, and hip joints, along with the coordinated actions of various muscle groups, are precisely controlled to ensure a stable, efficient, and adaptable pattern of locomotion. Any disruption to this complex interplay due to injury, disease, or ageing can lead to observable gait anomalies.

Clinical Significance of Gait Parameters Quantitative analysis of gait parameters provides objective measures that are clinically significant for diagnosing conditions, assessing disease severity, monitoring progression, evaluating treatment efficacy, and predicting health outcomes, particularly in older adults and individuals with neurological or musculoskeletal disorders. LiDAR-based systems offer the potential for precise measurement of these parameters in more naturalistic settings than traditional laboratory environments. Key spatio-temporal gait parameters and their clinical relevance include:

Key Gait Parameters for Clinical and Biomechanical Analysis

– **Gait Speed (Velocity):** The distance covered per unit of time (e.g., metres per second). It is a vital sign and strong predictor of functional decline, hospitalisation, fall risk, cognitive impairment, and mortality in older adults. Reduced gait speed is a common indicator of frailty and underlying pathology.
– **Step Length:** The distance between the initial contact point of one foot and that of the opposite foot. Asymmetrical or shortened step lengths may indicate neurological disorders (e.g., Parkinson's disease, stroke), pain, or muscle weakness.
– **Stride Length:** The distance between two successive initial contacts of the same foot. It includes two step lengths and is often reduced in individuals with slower gait speed.

- **Step Width (Base of Support):** The lateral distance between the midlines of both feet during double support. Increased step width may enhance stability and is often observed in patients with balance disorders, cerebellar ataxia, or fear of falling. Conversely, excessively narrow step width may reduce stability.
- **Cadence (Step Rate):** The number of steps taken per unit time (e.g., steps per minute). Variations in cadence may reflect compensatory mechanisms for gait impairments or underlying neurological conditions.
- **Stance Time:** The duration the foot remains in contact with the ground during one gait cycle. Prolonged stance time on one limb may indicate pain or contralateral limb instability.
- **Swing Time:** The duration the foot is off the ground during one gait cycle.
- **Double Support Time:** The period during which both feet are in contact with the ground. Increased double support time is often a compensatory mechanism to enhance stability, especially in older adults or individuals with impaired balance.
- **Gait Variability:** Refers to fluctuations in gait parameters such as step length and swing time between successive strides. High gait variability is associated with increased fall risk and is commonly observed in neurological conditions like Parkinson's disease and dementia.

Alterations in these parameters can signal various issues. For example, individuals with Parkinson's disease often exhibit a shuffling gait with reduced step length, reduced arm swing, and festination (involuntary acceleration of steps). Stroke survivors may show significant asymmetry in step length and swing time between the affected and unaffected limbs. LiDAR-based systems that can continuously and unobtrusively monitor these parameters in a home or clinical setting can provide valuable data for early detection of such anomalies, tracking disease progression, and tailoring rehabilitation strategies. The ability to collect data in a person's usual environment, as opposed to a formal laboratory, can lead to more ecologically valid assessments of their functional gait.

The following table summarises key spatio-temporal gait parameters and their clinical significance.

3 Experimental Setup

The preliminary assessment of the system was carried out using the Unitree 4D LiDAR L2 sensor, recognized for its precision and capability to capture intricate point cloud data. The following figure 1 displays the Unitree 4D LiDAR L2 sensor utilized in this study. The sensor was mounted at an elevated position in a controlled laboratory setting to obtain a thorough view of participants as they engaged in everyday activities such as walking, standing, and sitting.

The 3D point cloud data obtained from the LiDAR sensor offers a detailed depiction of the environment and the movements of participants. Figure 2 shows a sample illustration of this point cloud data, emphasizing a participant in motion within the captured scene. This visualization is a critical element for analyzing

Table 2: Key Spatiotemporal Gait Parameters and Their Clinical Significance

Gait Parameter	**Description**	**Typical Normal Range**	**Clinical Significance / Anomalies Indicated**
Gait Speed (Velocity)	Distance covered per unit time (e.g., m/s)	1.2 – 1.4 m/s	Reduced speed predicts fall risk, frailty, cognitive decline, and mortality. Increased speed may occur in hyperkinetic disorders.
Step Length	Distance from initial contact of one foot to the initial contact of the opposite foot	0.7 – 0.8 m	Reduced or asymmetrical step length may indicate Parkinson's disease, stroke, pain, or weakness.
Stride Length	Distance between two successive initial contacts of the same foot	1.4 – 1.6 m	Often reduced with slower gait speed; associated with elderly or pathological gait.
Step Width (Base of Support)	Lateral distance between midlines of the feet during double support	5 – 10 cm	Increased width: balance disorders, cerebellar ataxia, fear of falling. Decreased width may reduce stability or indicate scissor gait.
Cadence (Step Rate)	Number of steps per minute	100 – 120 steps/min	Altered cadence can reflect compensation or neurological issues. Lower in older adults or with pathology; higher in festinating gait (Parkinson's).
Stance Time	Duration foot is on the ground in one gait cycle	∼60% of gait cycle	Increased stance time may indicate ipsilateral limb issues or stability compensation. Asymmetry common after stroke or unilateral injury.
Swing Time	Duration foot is in the air during one gait cycle	∼40% of gait cycle	Decreased swing time is linked to increased stance time. Asymmetry may indicate unilateral limb impairment.
Double Support Time	Duration both feet are on the ground simultaneously	∼20% of gait cycle (10% initial, 10% terminal)	Increased in elderly, Parkinson's disease, or balance disorders. Reduced during fast walking or running.

Note: Typical normal ranges can vary based on age, sex, height, and individual factors. The values provided are general approximations for healthy adults.

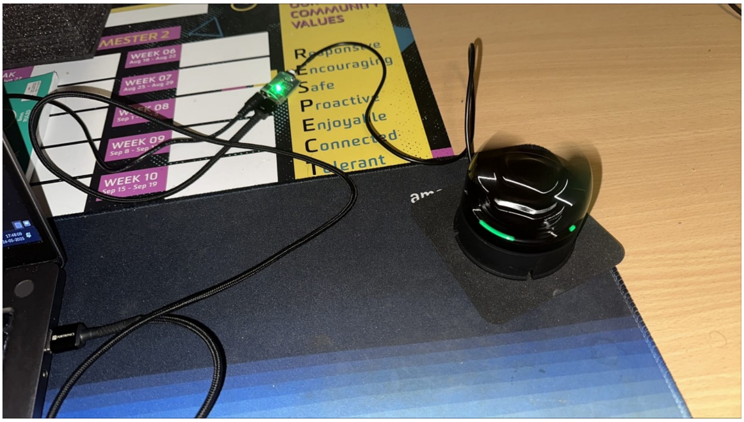

Fig. 1: Unitree 4D LiDAR L2 sensor

activities of daily living (ADLs) and plays a vital role in identifying anomalies and behavior patterns.

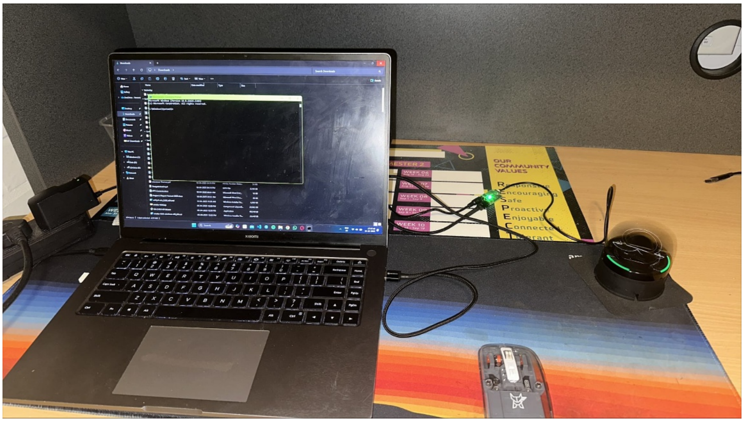

Fig. 2: Data Acquisition system

Data Collection Protocol: The LiDAR sensor consistently scanned the surroundings as participants carried out various ADLs. The data gathered was processed in real-time to create time-series data, which was subsequently analyzed for patterns and potential anomalies, as summarized in Table. Each activity was assessed based on metrics such as duration, frequency, and sequence, offering insights into any irregularities in the participants' behaviors. Preprocessing and Feature Extraction: Techniques for noise reduction were implemented to eliminate irrelevant data points, while segmentation algorithms differentiated human figures from the surrounding environment. Features in both the time-domain and frequency-domain were extracted from the processed data to input into the machine-learning models.

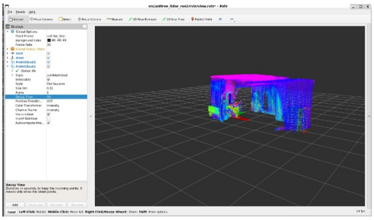

(a) Data Collection.

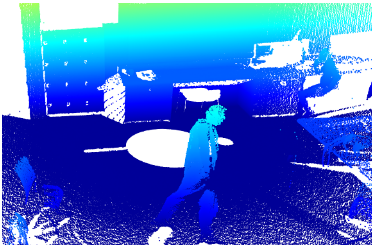

(b) Collected data.

Fig. 3: depiction of sample point cloud data showcasing a participant navigating through the immersive experimental environment

3.1 Experimental Evaluation The performance of the system was assessed through a series of practical tests, using quantitative metrics to evaluate both the accuracy of ADL classification and the system's ability to detect anomalies. The evaluation primarily concentrated on the following essential metrics:

ADL-Specific Metrics: The system's efficiency in correctly classifying Activities of Daily Living (ADLs) and identifying deviations from standard activity patterns was measured using metrics like accuracy, precision, recall, and F1-score. To examine classification performance and pinpoint misclassification trends, confusion matrices were utilized. These matrices proved particularly useful in evaluating instances where activities shared similar characteristics, such as differentiating between walking and standing.

Performance Metrics: The performance at the system level was assessed using several vital metrics, including latency, throughput, and resource utilization. Latency was evaluated by measuring the time lag between data acquisition and anomaly detection, offering insights into the system's responsiveness in real-time situations. Throughput was examined to determine the system's ability to efficiently handle large data streams, ensuring it can cope with the demands of continuous monitoring. Additionally, resource utilization was scrutinized to assess how effectively the edge computing and cloud infrastructure supported scalability, facilitating broader deployments of the system.

Data Analysis:Leveraging Deep Learning for Activity Recognition Human activity recognition utilizing LiDAR data poses unique challenges. This research proposes a deep learning methodology that employs Convolutional Neural Networks (CNNs) based architectures, such as 3D-CNN and PointNet, for accurate and effective classification of point clouds pertinent to the suggested indoor health monitoring system. Furthermore, we also explored the 3D object detection algorithm, COMPLEX 3D YOLO V4, to identify those cloud points that can assist in indoor health monitoring identification.

Data Pre-processing for Deep Learning: Pre-processing stages are critical to guarantee the quality and consistency of data for deep learning models. Techniques such as noise filtering, outlier removal, and normalization are employed to enhance model performance and generalizability. These steps are essential in optimizing model performance and its ability to generalize.

Noise Filtering: LiDAR data may be prone to noise due to sensor limitations or environmental impacts. Filtering techniques, like median filtering, can be utilized to eliminate noise and enhance data accuracy.

Outlier Removal: Outliers are data points that significantly differ from the majority of the data and can adversely affect the training process. Statistical methods or isolation techniques can be applied to identify and eliminate outliers from the LiDAR data.

Normalisation : Deep learning models typically operate better when the input data is normalised to a specified range. Normalisation techniques can be employed to scale the LiDAR data (e.g., X, Y, Z coordinates) to a defined range (e.g., 0 to 1 or -1 to 1) to boost training efficiency and convergence.

Point Cloud Classification with 3D CNNs: CNNs are proficient in extracting spatial features from data and have achieved success in various computer vision applications. In this instance, the 3D map created by the LiDAR sensor serves as a rich source of spatial information ideally suited for CNN analysis. In contrast to traditional 2D CNNs utilized for image recognition, 3D CNN architectures are purposely designed to handle and extract features from 3D data like point clouds produced by LiDAR sensors.

Point Cloud Classification with PointNet: Point clouds represent one of the primary types of geometrical data structure representation. Due to their irregular data structure, much research involves transforming such data into a regular format, such as 3D voxel grids, before inputting these point clouds into learning algorithms. However, PointNet introduces a neural network architecture that addresses the invariance among the input points. PointNet presents a straightforward and unified approach to effectively learn both local and global features from point clouds for various 3D recognition tasks. In our experiments, we are employing PointNet for classification purposes.

Point Clouds Detection with COMPLEX 3D YOLO V4: Complex YOLO is an effective object detection model that accurately estimates and localizes 3D multiclass bounding boxes. It operates on LiDAR-based bird's eye view RGB maps. The backbone architecture for Complex YOLOv4 is consistent with that of YOLOv2; however, it integrates E-RPN and complex angle regression to detect 3D objects precisely. The pre-processed RGB maps are input into the CNN network, and subsequently, E-RPN operates on the final feature map, simultaneously predicting the bounding boxes for each grid cell. E-RPN is a modified version of the commonly used Region Proposal Network (RPN) that performs well in angle regression for estimating 3D bounding boxes.

Model Training and Evaluation: We introduced a deep learning framework aimed at monitoring indoor activities, which was validated using the 3D object detection dataset from the KITTI Vision Benchmark Suite. The evaluation targeted Pedestrians and Cyclists, which are key categories related to the activities addressed by our framework. For the object detection task, we utilized the pre-established training, validation, and testing divisions from the KITTI dataset. We chose the KITTI dataset due to its robustness and exhaustive representation of real-world situations that correspond closely with the indoor activity patterns we wish to observe. This dataset offers high-quality 3D point cloud data, which is crucial for training models to detect and classify detailed human activities precisely. Furthermore, the standardized splits enable consistent and reliable benchmarking, ensuring our model's performance can be compared with recognized baselines. The detection algorithm was implemented using the hyperparameters and architecture with the model undergoing training for 300 epochs on an Nvidia 1080-Ti GPU. The 3D CNN and PointNet models were developed using Keras with TensorFlow, trained at a learning rate of 0.001, and reached convergence after 10 epochs. The 3D CNN consisted of three 3D convolutional layers followed by max-pooling layers. The training was conducted using TPU v2 resources via Google Colab. After preprocessing the data, the LiDAR information was applied to train the deep learning model.

3.2 Results and Discussion: The object detection efficiency of the proposed system was assessed using Mean Average Precision (mAP) at varying Intersection over Union (IoU) thresholds, as indicated in Tables II and III. Mean Average Precision (mAP) serves as a commonly adopted evaluation metric in object detection, calculating precision by determining the relevance of detected objects across all classes. Specifically, mAP@50 and mAP@75 were utilized, where the "50" and "75" indicate the IoU thresholds. mAP@50 evaluates the average precision when the predicted bounding box overlaps by at least 50% with the ground truth bounding box, whereas mAP@75 employs a more stringent threshold of 75% overlap. Table II displays the results of the system evaluated with mAP@50, while Table III presents the outcomes using mAP@75. Additionally, Tables IV and V illustrate the performance of the 3D Convolutional Neural Network (Conv3D) and PointNet architectures for classification tasks. These tables compare the accuracy of both models across the validation and test sets. Moreover, confusion matrices for the classification results of Conv3D and PointNet have been created to offer insights into the performance across different classes.

Table 3: Results on KITTI Test Set using Complex 3D Yolo v4 at IoU 0.5

Class	mAP	Precision	Recall	Mean Average Precision	F1
Pedestrian	0.88	0.65	0.92	0.77	0.76

Table 4: Results on KITTI Test Set using Complex 3D Yolo v4 at IoU 0.75

Class	mAP	Precision	Recall	Mean Average Precision	F1
Pedestrian	0.56	0.26	0.55	0.20	0.35

Table 5: Results on Test Set using PointNet

Class	Precision	Recall	F1
Pedestrian	0.93	0.50	0.65

4 Conclusion

The work presented acts as a proof of concept, highlighting the capacity of LiDAR technology to transform elderly care. Nonetheless, it is crucial to recognize that additional research and development are needed to fully explore the system's capabilities and tackle real-life obstacles. Empirical evidence shows that the system effectively classifies activities of daily living (ADLs) and identifies anomalies through machine learning algorithms. The user interface translates these functionalities into practical insights, facilitating real-time monitoring, activity tracking, and immediate notifications for caregivers. This proactive strategy promotes prompt interventions, minimizing risks related to independent living. Future efforts will aim to incorporate predictive analytics to automate responses, allowing for earlier identification of potential health concerns. Long-term studies with broader, diverse groups in real-world environments will further evaluate the system's sustained performance and address any existing challenges.

References

1. Purkis SJ, Brock JC. LiDAR overview. InCoral Reef Remote Sensing: A Guide for Mapping, Monitoring and Management 2013 Apr 19 (pp. 115-143). Dordrecht: Springer Netherlands.
2. Mehendale, N. and Neoge, S., 2020. Review on lidar technology. Available at SSRN 3604309.
3. Behroozpour, B., Sandborn, P.A., Wu, M.C. and Boser, B.E., 2017. Lidar system architectures and circuits. IEEE Communications Magazine, 55(10), pp.135-142.
4. International Electrotechnical Commission (IEC), 2014. IEC 60825-1: Safety of laser products – Part 1: Equipment classification and requirements. Geneva: International Electrotechnical Commission.
5. Günter, A., Böker, S., König, M. and Hoffmann, M., 2020, July. Privacy-preserving people detection enabled by solid state LiDAR. In 2020 16th international conference on intelligent environments (IE) (pp. 1-4). IEEE.
6. Ben-Shabat, Y., Shrout, O. and Gould, S., 2024. 3dinaction: Understanding human actions in 3d point clouds. In Proceedings of the IEEE/CVF Conference on Computer Vision and Pattern Recognition (pp. 19978-19987).
7. Rinchi, O., Ghazzai, H., Alsharoa, A. and Massoud, Y., 2023. LiDAR technology for human activity recognition: Outlooks and challenges. IEEE Internet of Things Magazine, 6(2), pp.143-150.
8. Simony, M., Milzy, S., Amendey, K. and Gross, H.M., 2018. Complex-yolo: An euler-region-proposal for real-time 3d object detection on point clouds. In Proceedings of the European conference on computer vision (ECCV) workshops (pp. 0-0).
9. Qi, C.R., Su, H., Mo, K. and Guibas, L.J., 2017. Pointnet: Deep learning on point sets for 3d classification and segmentation. In Proceedings of the IEEE conference on computer vision and pattern recognition (pp. 652-660).
10. Qi, C.R., Yi, L., Su, H. and Guibas, L.J., 2017. Pointnet++: Deep hierarchical feature learning on point sets in a metric space. Advances in neural information processing systems, 30.
11. Frøvik, N., Malekzai, B.A. and Øvsthus, K., 2021. Utilising LiDAR for fall detection. Healthcare Technology Letters, 8(1), pp.11-17.